Interaction of a partially fluorinated long-chain nicotinate with dipalmitoylphosphatidylcholine

Hans-Joachim Lehmler[1],* and **Paul M. Bummer[†]**

Department of Occupational and Environmental Health,* University of Iowa, Iowa City, IA 52242; and
College of Pharmacy,[†] University of Kentucky, Lexington, KY 40536

Abstract The interaction of a partially fluorinated long-chain nicotinate, F-NA18, a compound of interest as a chemopreventive agent, with dipalmitoylphosphatidylcholine (DPPC) was investigated in monolayers at the air-water interface and in fully hydrated bilayers and compared with its hydrocarbon analog, NA18. For the monolayer studies, the compression isotherms of mixtures of F-NA18 with DPPC were recorded at various compositions on a hydrochloric acid subphase (pH = 1.9–2.1, 32 ± 2°C). Analysis of the composition dependence of the average molecular area at constant film pressure and of the dependence of the breakpoints of the phase transitions suggests that F-NA18 is miscible with DPPC at the air-water interface, whereas NA18 shows some degree of immiscibility. In differential scanning calorimetry studies, only one major phase transition was observed for F-NA18-DPPC mixtures, whereas NA18-DPPC mixtures exhibited a complex phase behavior. The differences in the phase behavior of the respective mixtures may be the result of the geometric packing constraints of F-NA18 versus NA18.■ Therefore, for biomedical applications, the use of a partially fluorinated tail may offer advantages over simple hydrocarbon systems because, in addition to the chain length, the position and degree of fluorination can be adjusted.—Lehmler, H.-J., and P. M. Bummer. **Interaction of a partially fluorinated long-chain nicotinate with dipalmitoylphosphatidylcholine.** *J. Lipid Res.* 2005. **46:** 2415–2422.

Supplementary key words differential scanning calorimetry • Langmuir monolayer • liposomes • lipid phase transition • head-tail mismatch

Nicotinic acid and its alkyl esters are of considerable biological and pharmacological importance. Besides being the precursor of cofactors to many vital enzymes, nicotinic acid possesses vasodilating and fibrinolytic properties. Dietary supplements of nicotinic acid and dermatologic formulations of its long-chain esters are under investigation for the prevention and treatment of skin carcinogenesis (1). Nicotinic acid itself has been proven beneficial against bleomycin- and cyclophosphamide-induced lung injury in animal models (2–6). Because of the protective effect against lung injury mediated by reactive oxygen species, there is growing interest in the pulmonary administration of nicotinates, especially partially fluorinated nicotinates, using a perfluorocarbon vehicle (7, 8). In addition to their biological effects, nicotinates have been widely used as models to study drug uptake in vitro (9–12) and in vivo (9, 13–15). Because of their potential applications, the physicochemical characteristics, such as octanol-water partition coefficients and stability toward chemical and enzymatic degradation, have been well studied (8).

Despite the overall importance of nicotinates, little is known about the factors that determine the interaction of nicotinates with biological lipids, such as the phospholipids present in pulmonary surfactant. Studies of the phase behavior of long-chain nicotinates have shown partial miscibility with dipalmitoylphosphatidylcholine (DPPC) (16). Most notably, longer chain nicotinates, such as heptadecyl and octadecyl nicotinates, display a highly complex phase behavior with DPPC, which can be attributed to the head-tail mismatch that results from the larger cross-sectional area of the nicotinic acid head group [~26 square angstroms ($Å^2$)/molecule] versus the hydrophobic tail (~20 $Å^2$/molecule). Because of the great clinical potential of novel perfluorocarbon-based pulmonary drug-delivery systems (7, 8), it is also important to understand how the introduction of a perfluorinated segment into a long-chain nicotinate would affect the nicotinate-DPPC interaction. The introduction of such a perfluorinated segment into the hydrophobic tail of a long-chain nicotinate would likely introduce a strong dipole moment resulting from the CH_2CF_2 linkage and a larger cross-sectional area of the hydrophobic tail resulting from the larger van der Waals radius of the perfluoroalkyl group. Both factors are known to influence the phase behavior of mixtures of phosphatidylcholines with partially fluorinated long-chain carboxylic acids (17–19). The extent to which these factors would influence the phase behavior of fluorinated nicotinate-DPPC mixtures is not known.

[1] To whom correspondence should be addressed.
  e-mail: hans-joachim-lehmler@uiowa.edu

The aim of this study was to understand the extent to which the introduction of a perfluoroalkyl group alters the phase behavior of nicotinate-DPPC mixtures. For this purpose, we used a combination of monolayer and differential scanning calorimetry (DSC) studies to gain a better insight into the interaction of DPPC, an important biological phospholipid, and several long-chain nicotinates. Monolayer studies using DPPC at the air-water interface were chosen as a model of the pulmonary surfactant. This method allows the investigation of lipid mixtures and their miscibility at the air-water interface. DSC, on the other hand, is a straightforward tool to investigate the effect of the incorporation of organic compounds (e.g., nicotinates) into organic bilayers (16, 17). This technique allows the study of the effect of an interacting solute compound on the main lipid phase transition in a fully hydrated phospholipid bilayer membrane (20, 21). Changes in the onset of the so-called pretransition of phosphatidylcholines are another sensitive way to assess the interaction of an organic compound with a model lipid bilayer of this type of phospholipid. Overall, the combination of these two different approaches will further our understanding of phospholipid-nicotinate interactions and contribute to the rational design of fluorinated nicotinates for a variety of biomedical applications (8).
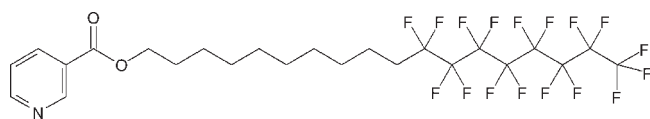
MATERIALS AND METHODS

Chemicals

DPPC was obtained from Avanti Polar Lipids in >99% purity and used without further purification. 2-Propanol, chloroform, methanol, octadecanol, and n-hexanes were HPLC grade and were purchased from Fisher Scientific or VWR. Concentrated hydrochloric acid was obtained from Fisher Scientific. Deionized water for the monolayer studies was distilled first from basic potassium permanganate followed by distillation from sulfuric acid (17–19, 22, 23). Deionized water for the DSC experiments was obtained from a Purelab Plus water system and had a resistance ≥ 18 Ω (16, 17).

Synthesis of long-chain nicotinates

The structure of F-NA18 (11,11,12,12,13,13,14,14,15,15,16,16,16-tridecafluorohexadecyl nicotinate) is shown in **Fig. 1**. The starting material for its synthesis, 11,11,12,12,13,13,14,14,15,15,16,16,16-tridecafluorohexadecan-1-ol, was synthesized using the methodology described previously (23). F-NA18 and its hydrocarbon analog, NA18, were synthesized from nicotinic acid and the corresponding alcohol according to literature procedures (8, 16, 24). In short, 1.1 equivalent of nicotinic acid was reacted with 1.0 equivalent of the corresponding alcohol in anhydrous dichloromethane using dicyclohexylcarbodiimide as a coupling reagent and dimethylaminopyridine as a catalyst. The esters were purified by column chromatography (silica gel, n-hexanes-ethyl acetate = 9:1) and recrystallized from methanol-chloroform. The purity of both esters was determined by gas chromatography. Both esters were purified to a purity of >99% based on relative peak area. The melting points of the nicotinates are given in **Table 1**.

Characterization of F-NA18

Yield = 51% of a white solid. ^{1}H-NMR (400 MHz, CDCl$_3$) δ 1.26–1.48 (12H, m), 1.54–1.63 (2H, m), 1.73–1.82 (2H, m), 1.96–2.11 (-CH$_2$CH_2CF$_2$-, 2H, m), 4.35 (-O-CH_2CH$_2$R, 2H, t, $^3J_{HH}$ = 6.8 Hz), 7.38 (-CH-, 1H, d, J = 8.0 Hz, d, J = 4.8 Hz, d, J = 0.8 Hz), 8.29 (-CH-, 1H, d, J = 8.0 Hz, "t", J = 2.0 Hz), 8.77 (-CH-, 1H, d, J = 4.8 Hz, d, J ~2.0 Hz), 9.22 (-CH-, 1H, "d", J = 1.2 Hz). ^{19}F-NMR (188 MHz, CDCl$_3$) δ −80.75 (-CF$_3$, 3F), −114.16 (-CF$_2$-, 2F), −121.61 (-CF$_2$-, 6F), −122.43 (-CF$_2$-, 2F), −123.25 (-CF$_2$-, 2F), −125.81 (-CF$_2$-, 2F). ^{13}C-NMR (100 MHz, CDCl$_3$) δ 20.05 (t), 25.95 (T), 28.60 (T), 29.18 (T, several C), 29.27 (T), 29.38 (T), 30.83 (T, t, $^2J_{CF}$ = 22.8 Hz), 65.54 (T), 123.25 (D), 126.33 (S), 137.00 (D), 150.90 (D), 153.33 (D), 165.34 (S). Mass spectrometry-electron ionization m/z (relative intensity): 681 (2), 680 (3, M-H), 662 (10, M-F), 248 (14), 206 (12), 164 (11), 124 (100), 107 (38), 106 (63), 79 (24), 78 (26), 69 (18), 56 (13), 55 (28). IR (KBr) [cm^{-1}]: 2,917, 2,852, 1,717, 1,288, 1,239, 1,205, and 1,147. Elemental analysis calculated for C$_{24}$H$_{24}$F$_{17}$O$_2$N: C 42.28, H 3.55, N 2.06; found: C 42.03, H 3.39, N 1.99.

Monolayer experiments

All monolayer experiments were carried out in a rectangular Teflon trough (306 × 150 mm) held at 37 ± 2°C (KSV-3000). The surface pressure was measured by the Wilhelmy plate method using paper plates (15 × 58 mm) as described previously (16–19, 22, 23, 25, 26). Every surface area-surface pressure isotherm was determined on a freshly poured subphase (hydrochloric acid, pH = 1.9–2.1). The subphase was allowed to equilibrate for 10 min at 37 ± 2°C. Surface-active impurities were removed from the air-water interface with a slight vacuum after compression of the barrier. Nicotinate, DPPC, and nicotinate-DPPC solutions with a concentration of 1–2 mg/ml were freshly prepared every day in n-hexanes-2-propanol (9:1). A known quantity of solution was spread on the surface, and 10 min at 37 ± 2°C was allowed to elapse for solvent evaporation before the start of the compression. A constant compression speed of 15 cm^2/min (10 mm/min) was used. Depending on the shape (i.e., collapse pressure) of the respective compression isotherm, the compression time was typically 15–20 min.

Preparation of samples for DSC

Calculated amounts of DPPC and nicotinate were dissolved in chloroform-methanol (3:1, v/v) at the appropriate mole fractions (16, 17, 26, 27). The solvent was removed under a stream of nitrogen, and the mixtures were further dried under vacuum for at least 3 h. The samples (either mixtures of phospholipids and nicotinate or pure phospholipid) were hydrated in an excess of water (three times by weight). Samples were heated above the lipid transition temperature for 5 min and vortexed for 2 min. This process was repeated four times. Finally, the samples were sonicated in a water bath above the lipid transition temperature for 30 min, followed by the heating and vortexing cycle mentioned above. Samples were stored at 4°C for 12–16 h. Hydration of samples was always carried out on the day before the DSC scans were collected. Samples of the neat nicotinate or nicotinate plus water (50% by weight) were weighed directly into the sample pan to determine the melting point of the nicotinates (Table 1).

A Thermal Analysis 2920 differential scanning instrument was used for the DSC studies. The hydrated samples were weighed into DSC aluminum pans. The DSC cell was purged with 60 ml/min, and the refrigerated cooling system was purged with 120

Fig. 1. Structure of F-NA18.

TABLE 1. Melting points of the neat nicotinates and the hydrated nicotinates (30% water) as determined by differential scanning calorimetry (22)

Nicotinate	Onset Temperature	Maximum Temperature	Melting Point (34)	Transitional Enthalpy
	°C			J/g
NA18 (neat)	54.15 ± 0.1	56.17 ± 0.1	55.3–55.8	200.35 ± 3.5
NA18 (hydrated)	53.49 ± 0.4	55.49 ± 0.4		197.63 ± 2.2
F-NA18 (neat)	46.42 ± 0.0	48.32 ± 0.1	Not reported	68.33 ± 0.6
F-NA18 (hydrated)	45.76 ± 1.0	48.30 ± 0.3		62.18 ± 5.8

ml/min, dry nitrogen. Samples were cooled to 4°C at a heating rate of 10°C/min and then heated from 4°C to 80°C at a heating rate of 5°C/min (17, 27, 28). All samples were subjected to two subsequent heating cycles. All experiments were carried out in triplicate. Onset, maximum, and offset temperatures, as well as peak width of the pretransition and the main phase transition, were determined for the second run using Universal Analysis NT software (16, 17, 22, 23, 26).

RESULTS

Behavior of long-chain nicotinates at the air-water interface

The present study investigates the mixing behavior of a partially fluorinated nicotinate (F-NA18) with DPPC in insoluble monolayers at the air-water interface. A hydrochloric acid subphase (pH = 1.9–2.1), although less relevant from a biological point of view, was chosen for this study to allow a comparison with previous studies of long-chain nicotinates (16) and other fluorinated compounds (17, 18, 22, 23, 26). As shown in **Fig. 2**, the compression isotherm of NA18 is of the condensed type, lacking a visible phase transition. On the other hand, the isotherm of F-NA18 exhibited a breakpoint characteristic of a phase transition from an expanded to a condensed state at 37°C. To verify that the breakpoint observed for F-NA18 is indeed the result of a phase transition, the compression isotherms of F-NA18 were recorded at different temperatures and the surface pressure at the onset of the phase transition was examined. As shown in **Table 2**, the onset of the phase transition of F-NA18 is temperature-dependent and is observed to vary over a fairly large temperature range (>20°C).

The limiting molecular area of each compression isotherm of F-NA18 was determined by extrapolating from the steep part of the compression isotherm to zero surface pressure. The limiting molecular area of F-NA18 is 34.0 Å^2/molecule at 37°C (Table 2). This is significantly greater than the limiting molecular area of hydrocarbon nicotinates (16). For example, NA18 has a limiting molecular area of 27.2 Å^2/molecule at 37°C.

Interaction at the air-water interface

The composition dependence of the onset of the phase transition of the compression isotherms was used as a criterion for the miscibility of binary mixtures at the air-water interface (17–19, 29, 30). In short, a composition-dependent phase transition onset is evidence of the complete miscibility of the components, whereas composition independence is a sign of immiscibility of the components (29). As a second criterion, the composition dependence of the average molecular area at constant film pressure may be used to assess the miscibility of two components at the air-water interface (17–19, 29, 30). In ideal behavior, the average area per molecule of any mixture is the weighted sum of the areas occupied by each species at the surface:

$$A(\pi) = X_{\text{Nicotinate}} \times A_{\text{Nicotinate}} + X_{\text{DPPC}} \times A_{\text{DPPC}} \quad (Eq.\ 1)$$

where X is the mole fraction of each component present at the air-water interface, A is the average area per molecule of the pure component, Nicotinate is the respective nicotinate, and DPPC is dipalmitoylphosphatidylcholine. This "additivity rule" gives the expected area per molecule,
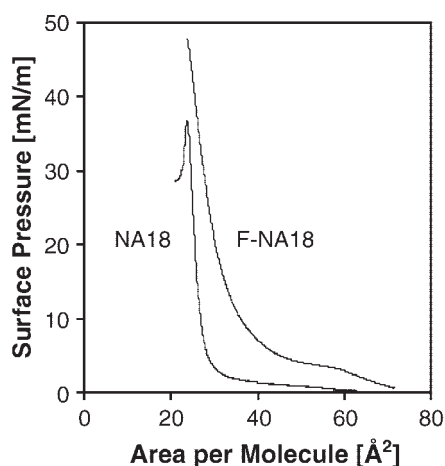

Fig. 2. Comparison of representative compression isotherms of F-NA18 and its hydrocarbon analog at 37°C on hydrochloric acid, pH = 1.9–2.1 Å^2, square angstroms.

TABLE 2. Temperature dependence of the π-A compression isotherms of F-NA18

Temperature	Limiting Molecular Area	Phase Transition
°C	square angstrom/molecule	mN/m
50.0	34.1 ± 0.3	7.4 ± 0.3
46.5	33.9 ± 1.3	6.2 ± 0.1
44.5	34.1 ± 0.2	5.2 ± 0.4
40.5	34.6 ± 1.4	4.2 ± 0.2
37.0	34.0 (n = 2)	3.1 ± 0.2
30.0	34.2 ± 1.0	1.5 ± 0.1

A(π), for ideal mixing or complete phase separation. Partial miscibility can be observed as a result of interaction between the two components. An attractive interaction will lead to a negative deviation of the experimental result compared with the ideal value calculated with equation 1, whereas a repulsive interaction will lead to a positive deviation from ideal behavior.

To investigate their mixing behavior, the compression isotherms of mixtures of F-NA18 with DPPC were recorded at various compositions at 37°C. **Figure 3** shows the compression isotherms and **Fig. 4** shows the onset of the respective phase transition from an expanded to a condensed phase of the F-NA18-DPPC and, for comparison, the NA18-DPPC mixtures. For the F-NA18-DPPC system, the liquid-expanded to liquid-condensed phase transition of DPPC occurs at an increasing surface pressure with increasing mole fraction of the partially fluorinated nicotinate (Figs. 3A, 4A). However, this phase transition cannot be observed for X(DPPC) < 0.6, and the compression isotherm at X(DPPC) = 0.4 shows only an expanded phase. At a high mole fraction of F-NA18 [i.e., X(DPPC) ⩽ 0.2], a phase transition from an expanded to a condensed phase can be observed at an increasing surface pressure. The analogous hydrocarbon system, NA18-DPPC, shows a distinctively different macroscopic phase behavior at the air-water interface (Figs. 3B, 4B). Although the onset pressure of the phase transition of pure DPPC initially increases with the decreasing mole fraction of DPPC, the onset pressure reaches a maximum at X(DPPC) ∼ 0.7–0.8 and appears to be constant starting at X(DPPC) ∼ 0.4. Furthermore, the compression isotherm at a mole fraction of X(DPPC) = 0.2 exhibits two distinct phase transitions, whereas no phase transition is observed for pure NA18.

The A-X diagrams of both the F-NA18-DPPC and NA18-DPPC systems are shown in **Fig. 5**. The A-X diagram of the F-NA18-DPPC system (Fig. 5A) nearly follows equation 1 at pressures between 10 and 20 mN/m. This observation provides additional evidence that the F-NA18-DPPC system is miscible at the air-water interface. In contrast, the A-X diagram of the hydrocarbon system at 10 mN/m exhibits a positive deviation from equation 1, thus suggesting that this system is partially miscible at this surface pressure. The A-X diagrams at other surface pressures are of limited use to assess the miscibility of the components in the composed film because of the presence of phase transitions (Fig. 4).

Interactions of F-NA18 and DPPC in an excess of water studied by DSC

In addition to the air-water interface, the present study investigates the mixing behavior of completely hydrated F-NA18-DPPC mixtures using DSC. The procedure for the preparation of the nicotinate-DPPC mixtures in excess water as well as the temperature program were similar to those in previous studies (17, 27, 28), thus allowing a direct comparison with the results from these investigations. Unfortunately, hydrochloric acid, which was used as subphase in the monolayer studies, cannot be used with DSC pans made from aluminum. Thus, a comparison between the monolayer and DSC studies is less direct. In an earlier study, we observed that nicotinate-DPPC mixtures show a complex phase behavior at mole fractions of DPPC < 0.7. This makes an interpretation of the phase diagrams at higher nicotinate concentrations difficult; therefore, we decided to concentrate our analysis on the biologically more relevant part of the phase diagrams with low F-NA18 concentrations [i.e., X(DPPC) > 0.5].

Figure 6 shows a comparison of the DSC thermograms of F-NA18 and its hydrocarbon analog NA18 at mole fractions of DPPC ranging from 1 down to 0.6. The partial phase diagrams of both mixtures are shown in **Fig. 7**. The comparison of both sets of DSC thermograms as well as the partial phase diagrams reveals several distinct differences between these mixtures. In the F-NA18-DPPC system, the onset temperature of the main phase transition decreases only slightly with increasing concentration of F-NA18 [up to X(DPPC) = 0.87] and remains constant at
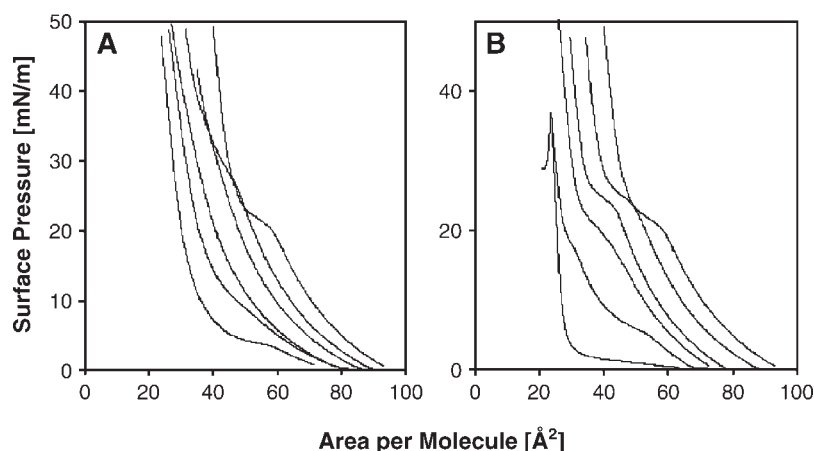
Fig. 3. Typical compression isotherms of mixtures of dipalmitoylphosphatidylcholine (DPPC) with F-NA18 (0, 0.2, 0.4, 0.6, 0.8, and 1) (A) and NA18 (0, 0.2, 0.4, 0.6, 0.8, and 1) (B) at 37°C on hydrochloric acid, pH = 1.9–2.1. Numbers in parentheses are the mole fractions of DPPC (from left to right).
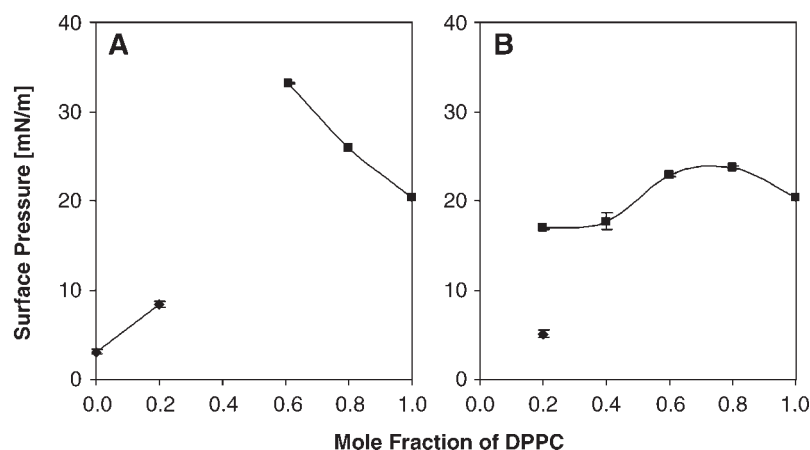
Fig. 4. Mole fraction dependence of the phase transition of mixtures of DPPC with F-NA18 (A) and NA18 (B) (37°C, hydrochloric acid, pH = 1.9–2.1). All data points are averages of at least three experiments ± 1 SD.

lower mole fractions of DPPC. The peak of the main transition of all F-NA18-DPPC mixtures is broader compared with pure DPPC, with a maximum half-width at approximately $X(DPPC) = 0.87$ (Fig. 7A). A much more complex phase behavior can be observed for the NA18-DPPC system (Fig. 7B). Most notable is the marked decrease of the onset of the main phase transition with increasing NA18 concentration, the significant peak broadening starting at $X(DPPC) = 0.77$, and the presence of several additional phase transitions at higher temperatures below mole fractions of DPPC ≤ 0.66. These additional phase transitions indicate the presence of NA18-rich lipid phase because they occur slightly below the melting point of pure NA18 (dotted line in Fig. 7B). In contrast, there is no evidence for the formation of similar F-NA18-rich phases down to $X(DPPC) < 0.68$.

A distinct pretransition peak can be observed for the F-NA18 mixture over the entire concentration range studied. The onset of the pretransition in this system occurs at a slightly lower temperature compared with fully hydrated DPPC, but it remains constant up to $X(DPPC) = 0.68$. In the NA18-DPPC system, the onset of the pretransition of

DPPC occurs at decreasing temperatures and displays significant peak broadening with increasing concentration. Below a mole fraction of DPPC = 0.91, the pretransition is finally abolished.

DISCUSSION

A hydrochloric acidic subphase with a pH of 1.9–2.1 was chosen for the monolayer studies to allow for a direct comparison with previous studies (16–19, 22, 23, 25, 26). The selection of this pH is partly justified by the fact that the lung fluid is acidic in certain types of lung disease. In addition, a recent study of the 10-(perfluorohexyl)-decanol-DPPC system revealed only slight differences in the macroscopic phase behavior of this system when determined on a water versus a hydrochloric acid subphase (25). This suggests that the mixing behavior of nicotinate-DPPC mixtures on a hydrochloric acid subphase is a good approximation of biologically more relevant conditions such as water at pH $\sim$ 7.
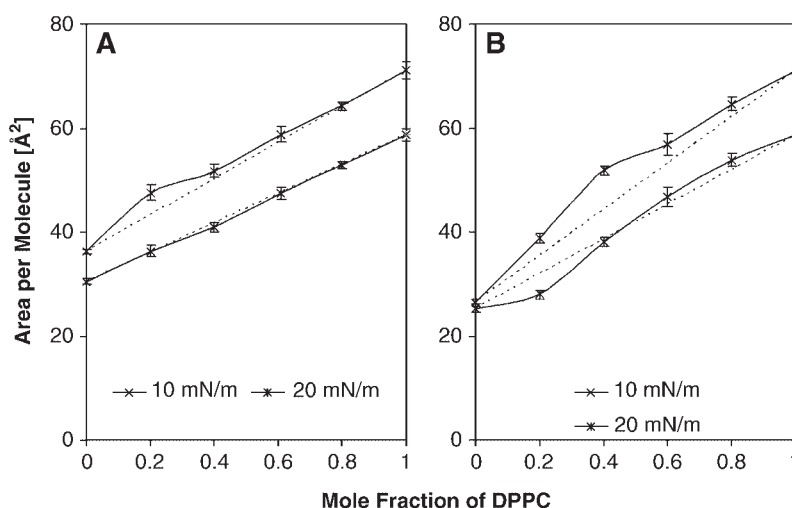
Fig. 5. A-X_{DPPC} diagrams of mixtures of DPPC with F-NA18 (A) and NA18 (B) (37°C, hydrochloric acid, pH = 1.9–2.1). The dotted lines indicate ideal behavior as defined by equation 1. All data points are averages of at least three experiments ± 1 SD.

Temperature [°C]
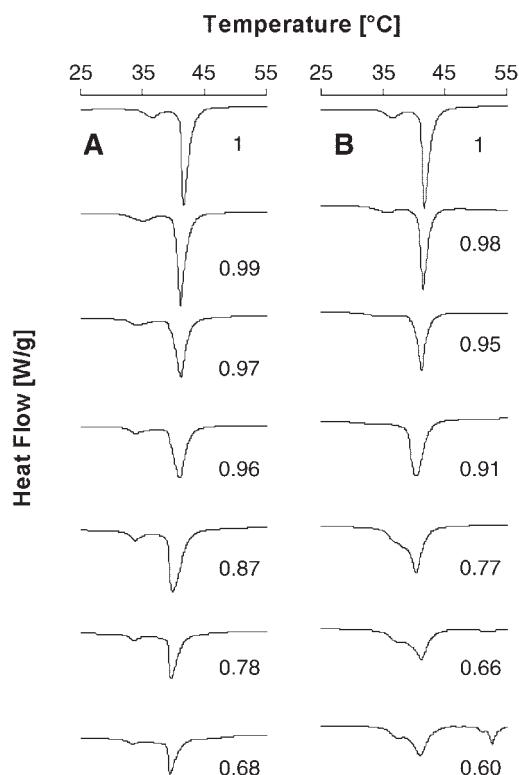
Fig. 6. Typical calorimetric scans for mixtures of DPPC with F-NA18 (A) and NA18 (B) in excess water. The mole fraction of DPPC is indicated beside each scan. The heating rate was 5°/min from 4°C to 80°C (only the part of the curve with a phase transition is shown).

Monolayer studies of pure F-NA18

As shown in Table 1, F-NA18 forms insoluble monolayers on a hydrochloric acid subphase over a wide temperature range. Its limiting molecular area is 34 Å^2/molecule at 37°C, which is similar to the limiting molecular area reported for other partially fluorinated amphiphiles (22, 23). The limiting area of the hydrocarbon nicotinate NA18 under identical experimental conditions is 27 Å^2/molecule, which reflects the size of the (protonated) nicotinic acid head group at the air-water interface (16). Thus, in contrast to the hydrocarbon nicotinates, in which the
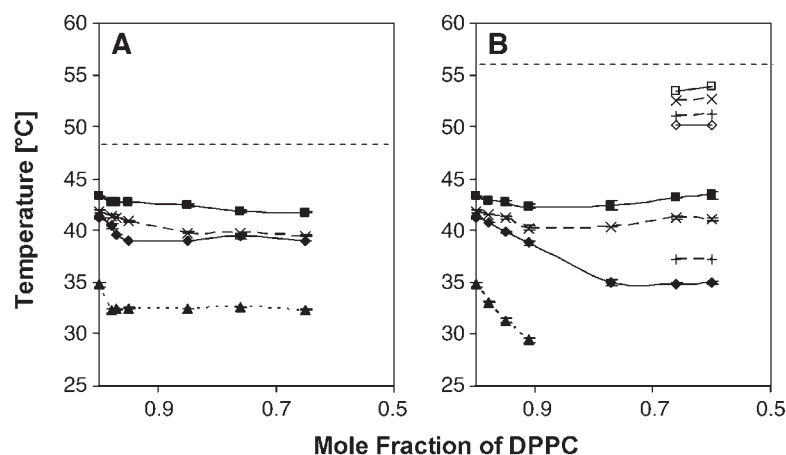
head group is larger compared with the hydrophobic tail (27 vs. 20 Å^2/molecule), F-NA18 shows an inverse head-tail mismatch, with the tail being larger than the head group (27 vs. 34 Å^2/molecule).

Compared with NA18, the inverse head-tail mismatch of F-NA18 is expected to result in significant differences in packing of the fluorinated tails and, ultimately, in the physical stability of the respective monolayers. As shown in Fig. 2, the compression isotherm of the partially fluorinated nicotinate exhibits a higher collapse pressure at 37°C. This is in contrast to monolayers of partially fluorinated carboxylic acids (22) and alcohols (23), in which the introduction of the highly polar CH$_2$CF$_2$ linkage and the combination of two tail segments with different cross-sectional areas (i.e., 20 Å^2 for alkyl vs. 30 Å^2 for perfluoroalkyl) causes packaging problems that result in a destabilization (i.e., a lower collapse pressure) of the monolayer of a partially fluorinated surfactant relative to its hydrocarbon analog. The higher collapse pressure of the F-NA18 monolayer compared with that of NA18 suggests that to some extent the larger cross-sectional area of the perfluoroalkyl terminus of the partially fluorinated nicotinate counteracts the destabilizing effect of the larger nicotinate head group.

As shown in Fig. 2 and Table 2, the compression isotherms of F-NA18 have a temperature-dependent transition from an expanded to a condensed phase. The phase transition of F-NA18 occurs over a relatively large temperature range of ∼20°C as well as a surface pressure range of ∼6 mN/m. T$_0$, the lowest temperature at which an expanded state can exist (31), was calculated to be 25.8°C using linear regression of the data points presented in Table 2. The shape of this phase transition is similar to that of the phase transition of similar fluorinated compounds but different from that of the characteristic first-order phase transition of hydrocarbon nicotinates at lower transition temperatures (16). The reason why no apparent first-order phase transition was observed for F-NA18 is probably attributable to the different packing of the partially fluorinated tail of F-NA18 at the air-water interface.

Monolayer studies of DPPC-nicotinate mixtures

Mixtures of long-chain hydrocarbon nicotinates are partially miscible at the air-water interface, with longer

Fig. 7. Partial phase diagram of mixtures of DPPC with F-NA18 (A) and NA18 (B) in excess water. Triangles, onset temperature of the pretransition; diamonds, onset temperature of the main transition; squares, offset temperature of the main transition. Times signs and plus signs represent maxima within a phase transition. The dotted line represents the melting point of the pure long-chain nicotinate. All data points are averages of at least three experiments ± 1 SD.

chain nicotinate such as NA18 being less miscible with DPPC (16). The F-NA18-DPPC system is also partially miscible at the air-water interface. However, in contrast to the NA18-DPPC system (Fig. 4B), the phase diagram of the F-NA18 system (Fig. 4A) is characterized by a phase transition that occurs at an increasing surface pressure with decreasing mole fraction of DPPC and, ultimately, is abolished. A similar trend of the phase transition has been reported for mixtures of DPPC with other long-chain compounds such as hexadecanol (32) and carboxylic acids (17, 18, 32). The phase behavior of the F-NA18 system, however, is quite different from that of other partially fluorinated compounds. For example, carboxylic acids and alcohols typically cause the opposite trend, that is, the phase transition of DPPC occurs at a decreasing surface pressure with decreasing mole fraction (17, 18, 25). The molecular origin of the distinct macroscopic phase behavior of F-NA18-DPPC is currently unknown but is likely a result of the overall molecular geometry of F-NA18 (i.e., its head-tail mismatch, with a larger limiting molecular area of the tail relative to the head group).

DSC studies

The F-NA18-DPPC system exhibits a less complex macroscopic phase behavior compared with NA18 (Figs. 6, 7). Some peak broadening of the main phase transition can be observed with increasing concentration of the partially fluorinated nicotinate. However, only one phase transition (plus a pretransition) can be observed down to mole fractions of DPPC of 0.68. There is no evidence of higher melting, nicotinate-rich phases over the entire concentration range studied. In contrast, the NA18-DPPC system displays several phase transitions, which indicates the presence of several different lipid assemblies. Most notably is the occurrence of nicotinate-rich lipid assemblies at higher concentrations of NA18 between the main gel-to-liquid phase transition of DPPC and the melting point of neat NA18 (Figs. 6B, 7B). The occurrence of nicotinate-rich phases at mole fractions of DPPC < 0.7 for NA18 suggests that NA18 has limited miscibility with DPPC, a conclusion that is in agreement with the monolayer studies (16).

The behavior of the main phase transition in the F-NA18-DPPC system suggests that F-NA18 is associated with the phospholipids and that the degree of association with DPPC appears to be much greater compared with the hydrocarbon nicotinate series. There are some similarities between the pentadecyl nicotinate-DPPC (16) and the F-NA18-DPPC systems. Despite a chain-length difference of three carbon atoms, both systems appear to be highly miscible over the entire concentration range studied. This observation is noteworthy because we have observed that partially fluorinated carboxylic acids resemble the behavior of shorter chain hydrocarbon acids at the air-water interface (22). The packaging constraints caused by the presence of the perfluorinated terminus and/or the CH_2CF_2 linkage may be responsible for this observation. However, to confirm this assessment, not only additional studies with a homologous series of partially fluorinated nicotinates but also studies

investigating the phase behavior of these mixtures on a molecular level are necessary.

DPPC and other phosphatidylcholines show a pretransition from a tilted to a vertical configuration, that is, a $L_{\beta'}$ (tilted gel) to $P_{\beta'}$ (ripple gel) phase transition (21). Mixtures of phosphatidylcholines with alkanes, alcohols, and carboxylic acids with a chain length of $\geqslant 12$ carbon atoms, as well as numerous small molecules and proteins, are known to reduce or eliminate the pretransition at low concentrations (33). Similarly, 11-(perfluorohexyl)-undecanoic acid, which is structurally similar to the tail of F-NA18, eliminates the pretransition of several phosphatidylcholines (17). In these systems, a more optimal (i.e., vertical) alignment of the tails is possible in the presence of small quantities of carboxylic acids and other small molecules, thus resulting in an elimination of the tilted gel phase and, hence, the pretransition. In contrast, a pretransition peak is present in the F-NA18-DPPC system over the entire concentration range, and the onset of these peaks appears to occur at the same temperature or at least in a similar temperature range (Fig. 7).

The changes in both the main transition and the pretransition suggest that F-NA18 is associated with DPPC. Based on our observation that F-NA18 also forms stable Langmuir monolayers at the air-water interface and therefore is surface-active, it is likely that the nicotinic acid head group is located at the water-lipid interface. Because of the inverse head-tail mismatch (i.e., because the partially fluorinated tail is larger compared with the head group), the packaging of the molecules in the F-NA18-DPPC bilayer is expected to be more favorable, thus resulting in a less complex phase behavior. However, it is also possible that the nicotinates are not aligned in the same manner as DPPC. Further studies are needed to fully characterize and understand the phase behavior and the underlying packaging constraints of DPPC-nicotinate mixtures.

Conclusions

Like hydrocarbon nicotinates such as NA18, F-NA18 is surface-active and forms stable monolayers at the air-water interface. It is miscible to a much greater extent, with DPPC in monolayers at the air-water interface as well as fully hydrated DPPC, compared with its hydrocarbon analog NA18. These observations are thought to be the result of the inverse head-tail mismatch of the partially fluorinated nicotinate (area head group < area tail) compared with hydrocarbon nicotinates (16). Overall, our experimental findings suggest that in both the monolayer and the fully hydrated DPPC, the nicotinates are oriented parallel to DPPC.

Our findings have implications for a variety of biomedical applications, such as pulmonary drug delivery of these compounds, as well as for understanding the biological effects of (long-chain) nicotinates. The present comparison between the hydrocarbon nicotinates and the partially fluorinated nicotinate F-NA18 shows that the introduction of a partially fluorinated tail significantly alters the influence of the nicotinate on the phase behavior of the DPPC-nicotinate mixtures. Therefore, the use of a partially fluori-

nated tail may offer advantages over simple hydrocarbon tails because not only the chain length but also the position and degree of fluorination can be readily adjusted. However, further studies are needed to fully use this exciting potential of partially fluorinated biological agents for pulmonary and other drug-delivery modalities.▪

REFERENCES

1. Jacobson, E. L., W. M. Shieh, and A. C. Huang. 1999. Mapping the role of NAD metabolism in prevention and treatment of carcinogenesis. *Mol. Cell. Biochem.* **193:** 69–74.
2. Gurujeyalakshmi, G., Y. Wang, and S. N. Giri. 2000. Suppression of bleomycin-induced nitric oxide production in mice by taurine and niacin. *Nitric Oxide.* **4:** 399–411.
3. Gurujeyalakshmi, G., Y. Wang, and S. N. Giri. 2000. Taurine and niacin block lung injury and fibrosis by down-regulating bleomycin-induced activation of transcription nuclear factor-kappaB in mice. *J. Pharmacol. Exp. Ther.* **293:** 82–90.
4. Giri, S. N., R. Blaisdell, R. B. Rucker, Q. Wang, and D. M. Hyde. 1994. Amelioration of bleomycin-induced lung fibrosis in hamsters by dietary supplementation with taurine and niacin: biochemical mechanisms. *Environ. Health Perspect.* **102:** 137–147.
5. Venkatesan, N., and G. Chandrakasan. 1994. In vivo administration of taurine and niacin modulate cyclophosphamide-induced lung injury. *Eur. J. Pharmacol.* **292:** 75–80.
6. Nagai, A., H. Matsumiya, M. Hayashi, S. Yasui, H. Okamoto, and K. Konno. 1994. Effects of nicotinamide and niacin on bleomycin-induced acute injury and subsequent fibrosis in hamster lungs. *Exp. Lung Res.* **20:** 263–281.
7. Lehmler, H-J., P. M. Bummer, and M. Jay. 1999. Liquid ventilation—a new way to deliver drugs to diseased lungs? *Chemtech.* **29:** 7–12.
8. Hsu, C-H., M. Jay, P. M. Bummer, and H-J. Lehmler. 2003. Chemical stability of esters of nicotinic acid intended for pulmonary administration by liquid ventilation. *Pharm. Res.* **20:** 918–925.
9. Guy, R. H., E. M. Carlstroem, D. A. W. Bucks, R. S. Hinz, and H. I. Maibach. 1986. Percutaneous penetration of nicotinates: in vivo and in vitro measurements. *J. Pharm. Sci.* **75:** 968–972.
10. Sugibayashi, K., T. Hayashi, K. Matsumoto, and T. Hasegawa. 2004. Utility of a three-dimensional cultured human skin model as a tool to evaluate the simultaneous diffusion and metabolism of ethyl nicotinate in skin. *Drug Metab. Pharmacokinet.* **19:** 352–362.
11. Ngawhirunpat, T., P. Opanasopit, and S. Prakongpan. 2004. Comparison of skin transport and metabolism of ethyl nicotinate in various species. *Eur. J. Pharm. Biopharm.* **58:** 645–651.
12. Rittirod, T., T. Hatanaka, A. Uraki, K. Hino, K. Katayama, and T. Koizumi. 1999. Species difference in simultaneous transport and metabolism of ethyl nicotinate in skin. *Int. J. Pharm.* **178:** 161–169.
13. Kompaore, F., J. P. Marty, and C. Dupont. 1993. In vivo evaluation of the stratum corneum barrier function in blacks, Caucasians and Asians with two noninvasive methods. *Skin Pharmacol.* **6:** 200–207.
14. Boelsma, E., C. Anderson, A. M. J. Karlsson, and M. Ponec. 2000. Microdialysis technique as a method to study the percutaneous penetration of methyl nicotinate through excised human skin, reconstructed epidermis, and human skin in vivo. *Pharm. Res.* **17:** 141–147.
15. Leopold, C. S., and B. C. Lippold. 1995. Enhancing effects of lipophilic vehicles on skin penetration of methyl nicotinate in vivo. *J. Pharm. Sci.* **84:** 195–198.
16. Lehmler, H-J., A. Fortis-Santiago, D. Nauduri, and P. M. Bummer. 2005. Interaction of long-chain nicotinates with dipalmitoylphosphatidylcholine. *J. Lipid Res.* **46:** 535–546.
17. Arora, M., P. M. Bummer, and H-J. Lehmler. 2003. Interaction of a partially fluorinated heptadecanoic acid with diacyl phosphatidylcholines of varying chain length. *Langmuir.* **19:** 8843–8851.
18. Lehmler, H-J., M. Jay, and P. M. Bummer. 2000. Mixing of partially fluorinated carboxylic acids and their hydrocarbon analogs with dipalmitoylphosphatidylcholine at the air-water interface. *Langmuir.* **16:** 10161–10166.
19. Lehmler, H-J., and P. M. Bummer. 2002. Mixing of partially fluorinated carboxylic acids with their hydrocarbon analogs at the air-water interface. *J. Colloid Interface Sci.* **249:** 381–387.
20. Silvius, J. R. 1991. Thermotropic properties of phospholipid analogues. *Chem. Phys. Lipids.* **57:** 241–252.
21. Huang, C-h., and S. Li. 1999. Calorimetric and molecular mechanics studies of the thermotropic phase behavior of membrane phospholipids. *Biochim. Biophys. Acta.* **1422:** 273–307.
22. Lehmler, H-J., M. O. Oyewumi, M. Jay, and P. M. Bummer. 2001. Behavior of partially fluorinated carboxylic acids at the air-water interface. *J. Fluorine Chem.* **107:** 141–146.
23. Lehmler, H-J., and P. M. Bummer. 2002. Behavior of 10-(perfluorohexyl)-decanol, a partially fluorinated analog of hexadecanol, at the air-water interface. *J. Fluorine Chem.* **117:** 17–22.
24. Morishita, S-i., T. Saito, Y. Hirai, M. Shoji, Y. Mishima, and M. Kawakami. 1988. Synthesis and hypolipidemic activity of 2-substituted isobutyric acid derivatives. *J. Med. Chem.* **31:** 1205–1209.
25. Lehmler, H-J., and P. M. Bummer. 2005. Mixing behavior of 10-(perfluorohexyl)-decanol and DPPC. *Colloids Surf. B. Biointerfaces.* **44:** 74–81.
26. Lehmler, H-J., and P. M. Bummer. 2004. Mixing of perfluorinated carboxylic acids with dipalmitoylphosphatidylcholine. *Biochim. Biophys. Acta.* **1664:** 141–149.
27. Koynova, R. D., A. I. Boyanov, and B. G. Tenchov. 1987. Gel-state metastability and nature of the azeotropic points in mixtures of saturated phosphatidylcholines and fatty acids. *Biochim. Biophys. Acta.* **903:** 186–196.
28. Eliasz, A. W., D. Chapman, and D. F. Ewing. 1976. Phospholipid phase transitions. Effects of *n*-alcohols, *n*-monocarboxylic acids, phenylalkyl alcohols and quarternary ammonium compounds. *Biochim. Biophys. Acta.* **448:** 220–230.
29. Dörfler, H-D. 1990. Mixing behavior of binary insoluble phospholipid monolayers. Analysis of the mixing properties of binary lecithin and cephalin systems by application of several surface and spreading techniques. *Adv. Colloid Interface Sci.* **31:** 1–110.
30. Motomura, K. 1974. Thermodynamics of multicomponent monolayers. I. General formulation. *J. Colloid Interface Sci.* **48:** 307–318.
31. Kellner, B. M. J., F. Müller-Landau, and D. A. Cadenhead. 1978. The temperature-dependence characterization of insoluble films at the air-water interface. *J. Colloid Interface Sci.* **66:** 597–601.
32. Lee, K. Y. C., A. Gopal, A. von Nahmen, J. A. Zasadzinski, J. Majewski, G. S. Smith, P. B. Howes, and K. Kjaer. 2002. Influence of palmitic acid and hexadecanol on the phase transition temperature and molecular packing of dipalmitoylphosphatidyl-choline monolayers at the air-water interface. *J. Chem. Phys.* **116:** 774–783.
33. Lohner, K. 1991. Effects of small organic molecules on phospholipid phase transitions. *Chem. Phys. Lipids.* **57:** 341–362.
34. Badgett, C. O., R. C. Provost, C. L. Ogg, and C. F. Woodward. 1945. Nicotinic acid. Water-insoluble esters and amides. *J. Am. Chem. Soc.* **67:** 1135–1138.